Blind Image Quality Assessment Based on Phase Congruency and Spatial-spectral Entropies

Maozheng Zhao, Yanping Lu, Cuiwei Li, Ran Gao, Qin Tu, Bo Yang, Aidong men

School of Information and Communication Engineering
Beijing University of Posts and Telecommunications
Beijing, 100876, China
{*maozhengzhao, luyanping, lcwhxzljj, gaoran, tuqin, boyang, menad*}*@bupt.edu.cn*

***Abstract*—We develop an efficient general-purpose blind image quality assessment (IQA) algorithm. It utilizes curvelet domain features of phase congruency (PC) values, local spatial entropy values and local spectral entropy values of distorted images as quality relevant features for quality prediction. A 2-stage framework including classification of distortion types and distortion specific quality assessment is utilized for mapping the quality relevant features to predictive scores. The classifier is implemented by a support vector machine (SVM) and the regression model is implemented by a support vector regression (SVR) model. The proposed approach which is named Phase Congruency and Spatial-Spectral Entropy based Quality (PCSSEQ) index can assess image quality blindly with out knowing the distorted type of the testing image and the predictive results of the proposed approach correlates well with human subjective scores. The performance of PCSSEQ on LIVE database is competitive with some state-of-the-art general-purpose blind image quality assessment (BIQA) approaches and some full-reference (FR) image quality assessment (IQA) approaches. We also prove that PCSSEQ has a good database independence characteristics.**

I. Introduction

Blind image quality assessment (BIQA) aims to build computational models that can evaluate image quality consistently with human perception without the undistorted version of the testing image. With the easier availability of digital images from the internet and the popularization of digital imaging devices such as smart phones with big screens and digital cameras, digital images have been becoming one of the most important way of representing and transmitting information in our everyday life. However, the perceptual quality of digital images may be declined by the process of acquisition, transmission, compression, restoration, etc. And in most cases the undistorted version of the observed image is not available, thus assessing image quality blindly has becoming increasingly important [1].

In terms of whether specifying the distortion types of testing images, the current BIQA methods can be classified as distortion specific methods [2], [3] or general purpose methods [4], [5], [6], [7], [8]. The application of distortion specific BIQA methods is limited by the necessity of knowing distortion types of testing images before quality assessment while the general-purpose BIQA approaches aim to predict quality of an image without any prior knowledge of the distortion type. Most general-purpose BIQA approaches proposed are based on training and learning. Moorthy and Bovik proposed a two-stage framework for BIQA [7] which first compute the probability of occurrence of each distortion type and then compute quality score on each distortion type, the two-stage framework performs well. They later proposed the DIIVINE index [6] which is also based on the two-stage framework and achieves better performance by utilizing natural scene statistics (NSS) features from wavelet domain. The BRISQUE index proposed by Mittal *et al.* extracts NSS features from the spatial domain which results in very low time complexity and superior performance [4]. L.Liu *et al.* proposed SSEQ [9] which applies curvelet domain statistical features, i.e. mean values and skew values of histograms of block-based spatial entropy and spectral entropy, as features. The 2-stage framework is also used for mapping features to quality scores, the performance of SSEQ is comparable to state-of-the-art BIQA methods.

However, the spatial entropy features (mean values and skew values of histograms of block-based spatial entropy) used in SSEQ performs poorly when utilized to the two-stage framework [7], [6]. In our work, we propose some new curvelet domain statistical features that performs significantly better for BIQA than spatial entropy features used in SSEQ. The new features are the mean values and the skew values of phase congruency (PC) histogram of an image. Although PC has already been applied for image quality assessment (IQA) in the literature [10], [11], [12], few of them utilize the curvelet domain statistical features of PC. Adding the proposed features to SSEQ framework results in a new BIQA which we call phase congruency and spatial-spectral entropy based quality (PCSSEQ) index. We thoroughly evaluated PCSSEQ on LIVE IQA database [13] and proved that PCSSEQ performs significantly better than SSEQ and its performance is comparable to several top-performing BIQA methods such as DIIVINE and BRISQUE, it also outperforms the two classical full reference (FR) IQA method PSNR [14] and SSIM [15] on LIVE database.

The rest of the paper is organized as follows. Section 2 describes details about the framework of PCSSEQ. In Section 3, we analyzed the power of quality prediction of each feature

This work is supported by the National Science Foundation of China (61271190).

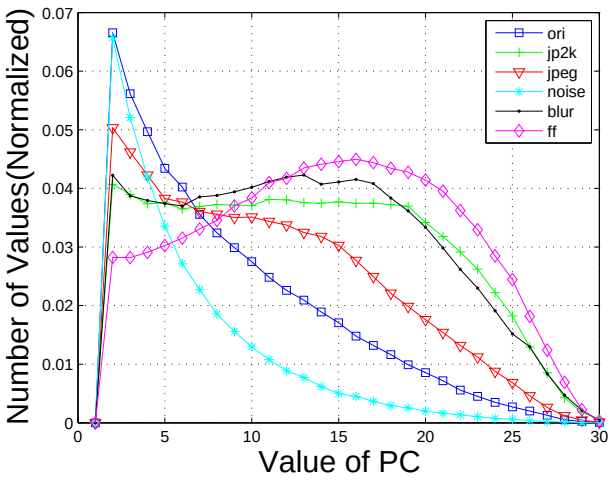

Fig. 1. Histograms of PC for different distortion types. The 6 curves correspond to the image "sailing4.bmp" and its distorted counterparts. "ori" (DMOS = 0), "jp2k" (DMOS = 64.7259), "jpeg" (DMOS = 64.6264), "noise" (DMOS = 63.7033), "blur" (DMOS = 53.3056), "ff" (DMOS = 71.6422).

subset used in PCSSEQ and evaluated the performance of PCSSEQ by several experiments. Finally, Section 4 concludes with a summary of our work.

II. BIQA BASED ON PHASE CONGRUENCY AND SPATIAL-SPECTRAL ENTROPIES

A. Phase congruency features

The physiological and psychophysical evidences had proved that visually discernable features coincide with points where the Fourier waves have congruent phases at different frequencies [16], [17], i.e., at points of high PC values. Besides, PC also have the characteristic of contrast invariance. Thus, the PC theory provides a simple but biologically plausible model of how mammalian visual systems detect and identify features in an image.

In this paper, we adopt the method of computing PC developed by Kovesi [17], which is widely used in literature. We adopt logarithmic Gabor filters [18] for wavelet transform and adopt Gaussian function as the spreading function for the log-Gabor filters to extend to 2D ones. The 2-D log-Gabor filters extended by Gaussian function have the following transfer function:

$$G_2(\omega,\theta_j)=\exp\left(-\frac{\left(\log(\frac{\omega}{\omega_0})\right)^2}{2\sigma_r^2}\right)\cdot\exp\left(-\frac{(\theta-\theta_j)^2}{2\sigma_\theta^2}\right), \tag{1}$$

where ω_0 is the filter's center frequency, and σ_r controls the filters bandwidth, $\theta_j = j\pi/J$, $j = \{0,1,...,J-1\}$ is the orientation angle of the filter, J is the number of orientations, and σ_θ determines the filter's angular bandwidth.

Denoted by M^e_{n,θ_j} and M^o_{n,θ_j} the even- and odd-symmetric filters of the 2-D log-Gabor filters on scale n and orientation θ_j, and they form a quadrature pair. By modulating ω_0 and θ_j and convolving G_2 with an image, we get a set of responses at each point x as $\lfloor e_{n,\theta_j}(x), o_{n,\theta_j}(x)\rfloor$, where $e_{n,\theta_j}(x)$ and $o_{n,\theta_j}(x)$ are responses of the quadrature pair on scale n and orientation θ_j at location x. The local amplitude on scale n and orientation θ_j is $A_{n,\theta_j}(x) = \sqrt{e_{n,\theta_j}(x)^2 + o_{n,\theta_j}(x)^2}$, and the local energy along orientation θ_j is $E_{\theta_j}(x) = \sqrt{F_{\theta_j}(x)^2 + H_{\theta_j}(x)^2}$, where $F_{\theta_j}(x) = \sum_n e_{n,\theta_j}(x)$ and $H_{\theta_j}(x) = \sum_n o_{n,\theta_j}(x)$. The 2-D PC at x is defined as follows:

$$PC(x)=\frac{\sum_j E_{\theta_j}(x)}{\lambda+\sum_n\sum_j A_{n,\theta_j}(x)} \tag{2}$$

where λ is a small positive constant to keep the fraction stable when all the Fourier amplitudes are very small. $PC(x)$ is a real number within $0-1$.

B. Phase congruency and spatial-spectral entropy based quality index

One reference image in LIVE database and its five distorted counterparts of different distorted types are chosen for showing their histograms. The histograms are shown in Fig. 1, numbers of zeros of histograms are excluded. We can see that the mean and skew values of PC histograms change with different distorted types and distorted extents. From the experiments in section III, we can prove that mean and skew values of PC histograms are strong features for BIQA.

The mean and skew values of spatial entropy histogram and spectral entropy histogram of a natural image would also change with different distorted types and distorted extents in a similar way. The process of computing spatial and spectral entropies are as follows.

The spatial entropy is

$$S=-\sum_x p(x)\log_2 p(x), \tag{3}$$

where x are the pixel luminance values, $p(x)$ is the empirical probability density of x.

The spectral entropy is

$$F=-\sum_i\sum_j P(i,j)\log_2 P(i,j), \tag{4}$$

where

$$P(i,j)=\frac{C(i,j)^2}{\sum_i\sum_j C(i,j)^2}, \tag{5}$$

where $P(i,j)$ is the spectral probability of normalized DCT coefficients $C(i,j)^2$,$i\neq 1$,$j\neq 1$ (DC is excluded).

We extracted mean and skew values of histograms of pixel based PC values, mean and skew values of histograms of block based spatial entropy values and mean and skew values of histograms of block based spectral entropy values as the feature vector of an image for quality assessment, the 2-stage framework proposed in [7], [6] is utilized to map feature vectors to predictive scores. The proposed BIQA method is

named Phase Congruency and Spatial-Spectral Entropy based Quality (PCSSEQ) index.

The proposed PCSSEQ can be divided into four steps:

1) Down sampling. Each incoming distorted image is down sampled twice with a factor of 2 yielding 3 scales of the incoming image, in our experiments we found that this multi scale strategy can enhance the overall performance.

2) Feature computing. PC values PC on pixels, spatial entropy values S and spectral entropy values F on 8×8 nonoverlapping neighboring blocks are computed for each scale.

3) Feature pooling. For each scale, by sorting PC, S and F values of an image in ascending order, the ordered sets $PC = (pc_1, pc_2, ..., pc_m)$, $S = (se_1, se_2, ..., se_n)$ and $F = (fe_1, fe_2, ..., fe_n)$ are yielded. Here pc_i, se_j and fe_k are PC values, local spatial entropies and local spectral entropies, m and n are the number of pixels and blocks respectively within each scale. Then percentile pooling is applied to PC, S and F based on the assumption that distortions only occur in a subset of pixels or blocks. Extracting the central 60% elements from PC, S and F yields $PCp = (pc_{\lfloor 0.2m \rfloor}, pc_{\lfloor 0.2m \rfloor+1}, ..., pc_{\lfloor 0.8m \rfloor})$, $Sp = (se_{\lfloor 0.2n \rfloor}, se_{\lfloor 0.2n \rfloor+1}, ..., se_{\lfloor 0.8n \rfloor})$ and $Fp = (fe_{\lfloor 0.2n \rfloor}, fe_{\lfloor 0.2n \rfloor+1}, ..., fe_{\lfloor 0.8n \rfloor})$. The mean values of PCp, Sp, Fp and the skew values of PC, S, F make up the final features of each scale:

$$f = (mean(PCp), skew(PC), mean(Sp), skew(S), mean(Fp), skew(F)). \quad (6)$$

4) Prediction. Each distorted image has a feature vector of $3 \times 6 = 18$ dimensions. A two-stage framework for BIQA is utilized to map the feature vector to the final image quality score. The two-stage framework used here is the same as that in [7], [6]. The first stage of the framework is to compute the probability of occurrence of each distorted type of the testing image. The second stage is to map feature vector to a quality score on each distorted type. Then the the dot product between the vector of the probability of occurrence of each distorted type and the vector of quality score on each distorted type is the final predictive score. We use a support vector machine (SVM) for classification and support vector regression (SVR) for regression [19], [20]. The SVM and SVR are implemented by the LIBSVM package [21] and the radial basis function (RBF) is used in both implementations.

III. Experiments and results

We tested the performance of PCSSEQ on the LIVE database [13], which consists of 29 reference images and their distorted versions. The database offers five different types of distortion, i.e., JPEG2k (JP2K), JPEG, white noise (WN), Gaussian blur (BLUR) and fast fading (FF). For each distortion type, distorted images of 5 to 6 different distorted levels of each reference image are offered. Difference Mean Opinion Score (DMOS) values of those images are available.

Two evaluation indexes are used to evaluate the performance of our model. The first one is the Spearman Rank Order Correlation Coefficient (SROCC) which is related to prediction monotonicity of a model. The second one is the Linear Correlation Coefficient (LCC) after non-linear mapping. LCC is considered as a measure of prediction accuracy of a model. The non-linear mapping function used in our experiments is the same as the one in [22]. A value close to 1 for SROCC and LCC indicates good performance.

TABLE I
Meaning of features.

Features	Feature description
f1-f3	Means of PC values for 1-3 scales
f4-f6	Skews of PC values for 1-3 scales
f7-f9	Means of spectral entropy values for 1-3 scales
f10-f12	Skews of spectral entropy values for 1-3 scales
f13-f15	Means of spatial entropy values for 1-3 scales
f16-f18	Skews of spatial entropy values for 1-3 scales

TABLE II
SROCC between feature values and DMOS.

	JP2K	JPEG	WN	BLUR	FF
f1	0.8638	0.7190	0.9510	0.9183	0.8104
f7	0.9052	0.9432	0.9462	0.9408	0.8323
f13	0.1081	0.6914	0.6392	0.4832	0.3234
f4	0.8720	0.7061	0.7970	0.9132	0.8244
f10	0.8405	0.8429	0.3768	0.8405	0.7671
f16	0.0630	0.6129	0.1453	0.3138	0.1807

A. Comparison of feature prediction power

We conducted two experiments to investigate the prediction power of the three feature subsets, i.e. phase congruency feature subset, the spectral entropy feature subset and the spatial entropy feature subset. The first experiment is to investigate the correlation between each feature subset and DMOS on LIVE database. The meaning of features are shown in Table I. The absolute values of SROCC between those feature values and the DMOS for distorted images in LIVE database are shown in Table II. We only computed the SROCC between DOMS and the features extracted from the original scale of images ($f1$,$f7$,$f13$,$f4$,$f10$ and $f16$) since the SROCC on other two scales shows similar regularity.

For mean values (f_1, f_7 and f_{13}), the mean value of spectral entropy of images (f_7) correlates best except on "WN" while the mean value of spatial entropy of images (f_{13}) correlates worst on each distorted type and the mean value of PC of images (f_1) correlates much better than mean value of spatial entropy (f_{13}). For skew values (f_4, f_{10} and f_{16}), the skew value of PC of images (f_4) correlates best except on "JPEG" distorted type while the spatial one (f_{16}) correlates worst on each distorted type. We can conclude that PC features (f_1, f_4) correlate much better than spatial entropy features (f_{13}, f_{16}) and is competitive with spectral entropy features (f_7, f_{10}).

We also applied each feature subset, i.e. phase congruency feature subset, the spectral entropy feature subset and the

TABLE III
MEDIAN SROCC AND LCC ACROSS 1000 TRAIN-TEST TRIALS FOR EACH FEATURE SUBSET.

	SROCC	LCC
f1-f6	0.7644	0.7770
f7-f12	0.8763	0.8757
f13-f18	0.7205	0.7211

spatial entropy feature subset, to the 2-stage framework respectively. 80% of the reference images and their distorted counterparts were randomly selected as the training set and the remaining 20% of the reference images and their distorted counterparts were used as the testing set, the median experimental results over 1000 iterations across all distortion types are shown in the first two columns of Table III. We use the realigned DMOS scores [22] of the LIVE database.

From Table III, we can observe that the spectral entropy features ($f_7 - f_{12}$) perform best while the spatial entropy features ($f_{13} - f_{18}$) perform worst and the PC features ($f_1 - f_6$) perform significantly better than the spatial entropy features ($f_{13} - f_{18}$).

B. Comparison with other IQA approaches

PCSSEQ utilizes all three feature subsets which are phase congruency features, spectral entropy features and spatial entropy features. We tested PCSSEQ on LIVE database and compared the performance of PCSSEQ with three FR IQA methods (PSNR[14], SSIM[15] and FSIM[11]) and three other BIQA methods (SSEQ[9], DIIVINE[6], and BRISQUE[4]). The SSEQ [9] compared here only utilize the spatial entropy feature subset and the spectral entropy feature subset to the 2-stage framework. For BIQA methods in our experiments, median results of 1000 train-test trails by randomly selecting 80% of reference images and their corresponding distorted versions as the training set and the rest images in the database as the testing set. For FR IQA methods, a random 20% test set selection for 1000 times is also performed for a fair comparison, and the median results of 1000 trials are reported. Only the distorted images in the database are used for training and testing in our experiments. The results are shown in Table IV. The top three values of SROCC and LCC across all distortion types ("ALL") are shown in boldface.

The SROCC and LCC of PCSSEQ are higher than that of SSEQ on each distortion type and across all distortion types ("ALL") except the LCC value on "JPEG". The SROCC values in the column indexed by "ALL" are higher than that of FR IQA methods PSNR and SSIM and higher than that of BIQA method DIIVINE. But it is lower than that of FSIM and BRISQUE noting that FSIM is a full-reference approach and BRISQUE is one of the state-of-the-art blind IQA approaches. The LCC values in the column indexed by "ALL" shows consistent results. Although the overall performance of the proposed PCSSEQ is slightly inferior than that of BRISQUE, it is significantly better than that of SSEQ because of utilizing extra PC features. The results also demonstrate that PC map of an image has great potential for blind IQA while most extant literatures only focus on its application for FR IQA.

TABLE V
RESULTS OF THE PAIRWISE T-TEST CONDUCTED BETWEEN SROCC VALUES OF 1000 TRAIN-TEST TRAILS OF DIFFERENT METHODS.

	PSNR	SSIM	FSIM	DIIVINE	BRISQUE	SSEQ	PCSSEQ
PSNR	0	-1	-1	-1	-1	-1	-1
SSIM	1	0	-1	1	-1	1	-1
FSIM	1	1	0	1	1	1	1
DIIVINE	1	-1	-1	0	-1	-1	-1
BRISQUE	1	1	-1	1	0	1	1
SSEQ	1	-1	-1	1	-1	0	-1
PCSSEQ	1	1	-1	1	-1	1	0

TABLE VI
MEDIAN CLASSIFICATION ACCURACY ACROSS 1000 TRAIN-TEST TRIALS.

	JP2K	JPEG	WN	BLUR	FF	**ALL**
SSEQ	65.7	86.5	100.0	66.7	46.7	72.8
PCSSEQ	71.4	91.9	100.0	66.7	43.3	74.7

C. Statistical significance and hypothesis testing

The student t-test results between compared BIQA methods for SROCC values of 1000 iterations are listed in Table V. A value of "1" in the table means that the mean value of SROCC of row method is statically higher to the column method, while a "-1" means that the mean value of SROCC of row method is statistically lower than the one in the column. A value of "0" means that the mean values of SROCC of row and column are statistically equivalent.

D. Classification accuracy

The median classification accuracy of 1000 train-test trails of SSEQ and PCSSEQ are listed in Table VI. From the table we can see that introduction of PC features slightly enhances the overall classification accuracy.

E. Database independence

TABLE VII
SROCC OBTAINED BY TRAINING ON THE LIVE IQA DATABASE AND TESTING ON THE TID2008 DATABASE.

	JP2K	JPEG	Noise	Blur	**ALL**
PSNR	0.7848	0.8585	0.9147	0.8914	0.7527
SSIM(SS)	0.9603	0.9354	0.8168	0.9598	0.9016
BRISQUE	0.9037	0.9102	0.8227	0.8742	0.8977
SSEQ	0.9112	0.8629	0.7986	0.8531	0.8501
PCSSEQ	0.9418	0.9168	0.8001	0.9106	0.9112

In order to demonstrate the degree of database independence of PCSSEQ, we trained it on the entire LIVE database and applied it to the TID2008 database [23]. The TID2008 database consists of 25 reference images and 1700 distorted images over 17 distortion categories. Of the 25 reference images only 24 are natural images, we test PCSSEQ on the 24 natural reference images only on distortions that are shared by the two

TABLE IV
MEDIAN SROCC AND LCC ACROSS 1000 TRAIN-TEST TRIALS ON THE LIVE IQA DATABASE. THE TOP THREE VALUES OF SROCC AND LCC ACROSS ALL DISTORTION TYPES ("ALL") ARE SHOWN IN BOLDFACE.

	SROCC						LCC					
	JP2K	JPEG	Noise	Blur	FF	**ALL**	JP2K	JPEG	Noise	Blur	FF	**ALL**
PSNR	0.8673	0.8843	0.9428	0.7575	0.8721	0.8633	0.8657	0.8866	0.8963	0.7855	0.8616	0.8568
SSIM(SS)	0.9395	0.9480	0.9644	0.9083	0.9413	0.9129	0.9513	0.9605	0.9828	0.9033	0.9569	0.9057
FSIM	0.9700	0.9807	0.9662	0.9711	0.9511	**0.9636**	0.9139	0.9833	0.9751	0.9681	0.9465	**0.9581**
DIIVINE	0.8907	0.8960	0.9826	0.9335	0.8396	0.9057	0.8961	0.9074	0.9765	0.9270	0.8541	0.8990
BRISQUE	0.9095	0.9647	0.9778	0.9511	0.8759	**0.9364**	0.9122	0.9735	0.9848	0.9456	0.9013	**0.9386**
SSEQ	0.8994	0.9420	0.9591	0.9172	0.8565	0.9122	0.9033	0.9609	0.9642	0.9286	0.8746	0.9158
PCSSEQ	0.9132	0.9461	0.9675	0.9246	0.8652	**0.9259**	0.9110	0.9477	0.9744	0.9377	0.8867	**0.9258**

databases: JP2K, JPEG, Gaussian noise (Noise), and Gaussian blur (Blur). The results are shown in Table VII. The SROCC between DMOS and the predictive scores of PCSSEQ is the highest compared with PSNR, SSIM, BRISQUE and SSEQ and it is even higher than that of BRISQUE. The results means that PCSSEQ has excellent database independence characteristic. The reason for the excellent database independence characteristic is probably that the features of PCSSEQ are statistical features of histograms of an entire image, those features are not easily affected by the sizes and the contents of the distorted images.

IV. CONCLUSION

We proposed a general-purpose BIQA approach called Phase Congruency and Spatial-Spectral Entropy based Quality (PCSSEQ) index. The curvelet domain statistical PC features proposed in our work shows strong predictive ability for BIQA. The proposed approach performs significantly better than another curvelet statistical feature based BIQA method SSEQ on LIVE database. The performance of PCSSEQ is also competitive with some state-of-the-art BIQA methods such as BRISQUE, DIIVINE and some FR IQA methods such as PSNR and SSIM. PCSSEQ also has a good database independence characteristic. Moreover, our work indicate that PC map of an image has great potential for BIQA while most extant literatures only focus on its application for FR IQA.

REFERENCES

[1] Z. Wang, "Applications of objective image quality assessment methods [applications corner]," *Signal Processing Magazine, IEEE*, vol. 28, no. 6, pp. 137–142, 2011.

[2] Z. Wang, H. R. Sheikh, and A. C. Bovik, "No-reference perceptual quality assessment of jpeg compressed images," in *Image Processing. 2002. Proceedings. 2002 International Conference on*, vol. 1. IEEE, 2002, pp. I–477.

[3] L. Meesters and J.-B. Martens, "A single-ended blockiness measure for jpeg-coded images," *Signal Processing*, vol. 82, no. 3, pp. 369–387, 2002.

[4] A. Mittal, A. K. Moorthy, and A. C. Bovik, "No-reference image quality assessment in the spatial domain," *Image Processing, IEEE Transactions on*, vol. 21, no. 12, pp. 4695–4708, 2012.

[5] P. Ye, J. Kumar, L. Kang, and D. Doermann, "Unsupervised feature learning framework for no-reference image quality assessment," in *Computer Vision and Pattern Recognition (CVPR), 2012 IEEE Conference on*. IEEE, 2012, pp. 1098–1105.

[6] A. K. Moorthy and A. C. Bovik, "Blind image quality assessment: From natural scene statistics to perceptual quality," *Image Processing, IEEE Transactions on*, vol. 20, no. 12, pp. 3350–3364, 2011.

[7] ——, "A two-step framework for constructing blind image quality indices," *Signal Processing Letters, IEEE*, vol. 17, no. 5, pp. 513–516, 2010.

[8] P. Ye and D. Doermann, "No-reference image quality assessment using visual codebooks," *Image Processing, IEEE Transactions on*, vol. 21, no. 7, pp. 3129–3138, 2012.

[9] L. Liu, B. Liu, H. Huang, and A. C. Bovik, "No-reference image quality assessment based on spatial and spectral entropies," *Signal Processing: Image Communication*, vol. 29, no. 8, pp. 856–863, 2014.

[10] R. Hassen, Z. Wang, and M. Salama, "No-reference image sharpness assessment based on local phase coherence measurement," in *Acoustics Speech and Signal Processing (ICASSP), 2010 IEEE International Conference on*. IEEE, 2010, pp. 2434–2437.

[11] L. Zhang, D. Zhang, and X. Mou, "Fsim: a feature similarity index for image quality assessment," *Image Processing, IEEE Transactions on*, vol. 20, no. 8, pp. 2378–2386, 2011.

[12] Z. Liu and R. Laganière, "Phase congruence measurement for image similarity assessment," *Pattern Recognition Letters*, vol. 28, no. 1, pp. 166–172, 2007.

[13] H. Sheikh, Z. Wang, L. Cormack, and A. Bovik, "Live image quality assessment database release 2," 2006, available from: http://live.ece.utexas.edu/research/quality.

[14] Z. Wang and A. C. Bovik, "Mean squared error: love it or leave it? a new look at signal fidelity measures," *Signal Processing Magazine, IEEE*, vol. 26, no. 1, pp. 98–117, 2009.

[15] Z. Wang, A. C. Bovik, H. R. Sheikh, and E. P. Simoncelli, "Image quality assessment: from error visibility to structural similarity," *Image Processing, IEEE Transactions on*, vol. 13, no. 4, pp. 600–612, 2004.

[16] M. C. Morrone and D. Burr, "Feature detection in human vision: A phase-dependent energy model," *Proceedings of the Royal Society of London. Series B, biological sciences*, pp. 221–245, 1988.

[17] P. Kovesi, "Image features from phase congruency," *Videre: Journal of computer vision research*, vol. 1, no. 3, pp. 1–26, 1999.

[18] D. J. Field, "Relations between the statistics of natural images and the response properties of cortical cells," *JOSA A*, vol. 4, no. 12, pp. 2379–2394, 1987.

[19] B. Schölkopf, A. J. Smola, R. C. Williamson, and P. L. Bartlett, "New support vector algorithms," *Neural computation*, vol. 12, no. 5, pp. 1207–1245, 2000.

[20] C. J. Burges, "A tutorial on support vector machines for pattern recognition," *Data mining and knowledge discovery*, vol. 2, no. 2, pp. 121–167, 1998.

[21] C.-C. Chang and C.-J. Lin, "LIBSVM: A library for support vector machines," *ACM Transactions on Intelligent Systems and Technology*, vol. 2, pp. 27:1–27:27, 2011, software available at http://www.csie.ntu.edu.tw/ cjlin/libsvm.

[22] H. R. Sheikh, M. F. Sabir, and A. C. Bovik, "A statistical evaluation of recent full reference image quality assessment algorithms," *Image Processing, IEEE Transactions on*, vol. 15, no. 11, pp. 3440–3451, 2006.

[23] N. Ponomarenko, V. Lukin, A. Zelensky, K. Egiazarian, M. Carli, and F. Battisti, "Tid2008-a database for evaluation of full-reference visual quality assessment metrics," *Advances of Modern Radioelectronics*, vol. 10, no. 4, pp. 30–45, 2009.